PERGAMON

International Journal of Heat and Mass Transfer 41 (1998) 3501–3513

International Journal of HEAT and MASS TRANSFER

Laminar mixed convection with viscous dissipation in a vertical channel

Antonio Barletta*

Dipartimento di Ingegneria Energetica, Nucleare e del Controllo Ambientale (DIENCA), Università di Bologna, Viale Risorgimento 2, I-40136 Bologna, Italy

Received 29 September 1997; in final form 13 January 1998

Abstract

Combined free and forced convection flow in a parallel-plate vertical channel is analysed in the fully developed region by taking into account the effect of viscous dissipation. The two boundaries are considered as isothermal and kept either at equal or at different temperatures. The velocity field, the temperature field and the Nusselt numbers are obtained by a perturbation series method which employs a perturbation parameter proportional to the Brinkman number. Dimensionless coefficients which allow the evaluation of the dimensionless mean velocity, of the dimensionless bulk temperature and of the Nusselt numbers are determined. © 1998 Elsevier Science Ltd. All rights reserved.

Nomenclature

A constant defined by equation (6) [Pa m^{-1}]
a_n, b_n dimensionless coefficients defined by equation (47)
Br Brinkman number defined in equation (12)
c_p specific heat at constant pressure [J kg^{-1} K^{-1}]
c_n, d_n dimensionless coefficients defined by equations (50) and (51), respectively
D $= 2L$, hydraulic diameter [m]
$\boldsymbol{g}$ acceleration due to gravity [m s^{-2}]
Gr Grashof number defined in equation (12)
j non-negative integer number
k thermal conductivity [W m^{-1} K^{-1}]
L channel width [m]
n non-negative integer number
Nu_-, Nu_+ Nusselt numbers defined by equation (24)
$\widehat{Nu}_-$, $\widehat{Nu}_+$ Nusselt numbers defined by equation (25)
p pressure [Pa]
P $= p+\rho_0 \boldsymbol{g} X$, difference between the pressure and the hydrostatic pressure [Pa]
Pr Prandtl number defined in equation (12)
Re Reynolds number defined in equation (12)
R_T temperature difference ratio defined in equation (12)
T temperature [K]
T_1, T_2 prescribed boundary temperatures [K]
T_0 reference temperature defined in equation (13)
u dimensionless velocity component in the X-direction defined in equation (12)
$u_n(y)$ dimensionless functions defined by equation (36)
$\bar{u}$ mean value of u defined in equation (16)
U velocity component in the X-direction [m s^{-1}]
U_0 reference velocity defined in equation (13)
$\mathbf{U}$ velocity [m s^{-1}]
X streamwise coordinate [m]
y dimensionless transverse coordinate defined in equation (12)
Y transverse coordinate [m].

Greek symbols

α $= k/(\rho_0 c_p)$, thermal diffusivity [m^2 s^{-1}]
β thermal expansion coefficient [K^{-1}]
ΔT reference temperature difference defined either by equation (14) or by equation (15)
ε dimensionless parameter defined by equation (35)
θ dimensionless temperature defined by equation (12)
θ_b dimensionless bulk temperature defined by equation (17)
μ dynamic viscosity [Pa s]
ν $= \mu/\rho_0$, kinematic viscosity [m^2 s^{-1}]
Ξ dimensionless parameter defined by equation (12)

* Corresponding author.

0017–9310/98 $19.00 © 1998 Elsevier Science Ltd. All rights reserved
PII: S0017–9310(98)00074–X

Ξ_c critical value of Ξ for the onset of flow reversal
ρ mass density [kg m^{-3}]
ρ_0 value of the mass density when $T = T_0$ [kg m^{-3}].

1. Introduction

Many analyses of combined forced and free convection flow in a parallel-plate vertical channel are available in the literature. A comprehensive review of the literature on this subject can be found in Aung [1]. Analytical and numerical solutions for the temperature and the velocity field have been obtained both for prescribed wall temperatures and for prescribed wall heat fluxes. However, all these theoretical studies are based on the hypothesis that the effect of viscous dissipation in the fluid is negligible.

One of the earliest analyses of laminar and fully developed mixed convection in a parallel-plate vertical channel with prescribed uniform temperatures at the boundaries can be found in Tao [2]. More recent investigations on this subject are presented in Aung and Worku [3], in Cheng et al. [4] and in Hamadah and Wirtz [5]. These authors point out that the temperature distribution in the fluid is uniform when both boundaries are at the same temperature (symmetric heating) and is a linear function of the transverse coordinate when the boundaries are kept at different temperatures (asymmetric heating). Therefore, in the case of asymmetric heating, heat transfer between the two boundaries of the channel occurs by pure conduction (conduction regime). Moreover, the buoyancy force influences the velocity profile and can give rise to flow reversal both for upward flow and for downward flow.

In the literature, both for prescribed wall temperatures and for prescribed wall heat fluxes, the analyses of fully developed mixed convection are performed by analytical methods, while the developing flow is analyzed by numerical techniques [6–8].

The aim of this paper is to extend the studies available in the literature on laminar and fully developed mixed convection in a parallel-plate vertical channel with prescribed wall temperatures, by taking into account the effect of viscous dissipation. This effect is expected to be relevant for fluids with high values of the dynamic viscosity as well as for high-velocity flows. Indeed, when viscous dissipation cannot be neglected, the temperature field is dependent on the velocity field through a nonlinear term in the energy balance equation. This coupling term is absent when viscous dissipation is neglected. In the case of asymmetric heating, a consequence of this coupling is that no conduction regime is present when viscous dissipation is taken into account. In the present paper, the temperature profile and the velocity profile are obtained by a perturbation method based on the perturbation parameter $Br\,Gr/Re$, where Br is the Brinkman number, Gr is the Grashof number and Re is the Reynolds number.

2. Governing equations

In this section, the momentum balance equation and the energy balance equation are written in a dimensionless form. Then, the solutions of these equations in the case of negligible viscous dissipation and in the case of forced convection are outlined.

Let us consider a Newtonian fluid which steadily flows in a parallel-plate vertical channel. The thermal conductivity, the thermal diffusivity, the dynamic viscosity and the thermal expansion coefficient are considered as constant. Moreover, the Boussinesq approximation as well as the equation of state

$$\rho = \rho_0[1-\beta(T-T_0)] \tag{1}$$

are supposed to hold. The choice of the spatial coordinates is described in Fig. 1. In particular, the X-axis is parallel to the gravitational field, but with the opposite direction. It is assumed that the only nonzero component of the velocity field $\mathbf{U}$ is the X-component U. Thus, as a consequence of the mass balance equation, one obtains

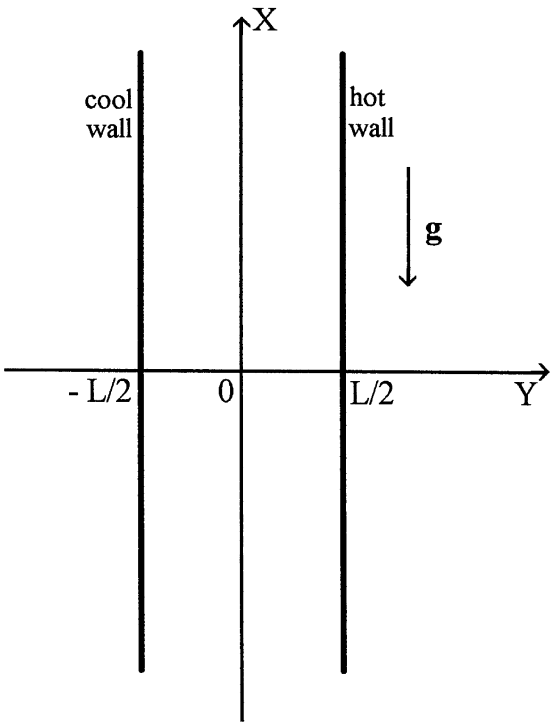

Fig. 1. Drawing of the system and of the coordinate axes.

$$\frac{\partial U}{\partial X}=0 \tag{2}$$

so that U depends only on Y. The streamwise and the transverse momentum balance equations yield [9]

$$\beta \boldsymbol{g}(T-T_0)-\frac{1}{\rho_0}\frac{\partial P}{\partial X}+\nu\frac{\mathrm{d}^2U}{\mathrm{d}Y^2}=0 \tag{3}$$

$$\frac{\partial P}{\partial Y}=0 \tag{4}$$

where $P=p+\rho_0 \boldsymbol{g} X$ is the difference between the pressure and the hydrostatic pressure. On account of equation (4), P depends only on X so that equation (3) can be rewritten as

$$\beta \boldsymbol{g}(T-T_0)-\frac{1}{\rho_0}\frac{\mathrm{d}P}{\mathrm{d}X}+\nu\frac{\mathrm{d}^2U}{\mathrm{d}Y^2}=0. \tag{5}$$

Let us assume that the walls of the channel are isothermal. In particular, the temperature of the boundary $Y=-L/2$ is T_1, while the temperature at $Y=L/2$ is T_2, with $T_2 \geqslant T_1$. These boundary conditions are compatible with equation (5) if and only if $\mathrm{d}P/\mathrm{d}X$ is independent of X. Therefore, there exists a constant A such that

$$\frac{\mathrm{d}P}{\mathrm{d}X}=A. \tag{6}$$

On account of equation (6), by evaluating the derivative of equation (5) with respect to X, one obtains

$$\frac{\partial T}{\partial X}=0 \tag{7}$$

so that also the temperature depends only on Y.

By taking into account the effect of viscous dissipation, the energy balance equation can be written as [9]

$$\alpha\frac{\mathrm{d}^2T}{\mathrm{d}Y^2}+\frac{\nu}{c_\mathrm{p}}\left(\frac{\mathrm{d}U}{\mathrm{d}Y}\right)^2=0. \tag{8}$$

Equations (5) and (8) allow one to obtain a differential equation for U, namely

$$\frac{\mathrm{d}^4U}{\mathrm{d}Y^4}=\frac{\beta \boldsymbol{g}}{\alpha c_\mathrm{p}}\left(\frac{\mathrm{d}U}{\mathrm{d}Y}\right)^2. \tag{9}$$

The boundary conditions on U are both the no slip conditions

$$U(-L/2)=U(L/2)=0 \tag{10}$$

and those induced by the boundary conditions on T and by equations (5) and (6), namely

$$\left.\frac{\mathrm{d}^2U}{\mathrm{d}Y^2}\right|_{Y=-L/2}=\frac{A}{\mu}-\frac{\beta \boldsymbol{g}(T_1-T_0)}{\nu},$$

$$\left.\frac{\mathrm{d}^2U}{\mathrm{d}Y^2}\right|_{Y=L/2}=\frac{A}{\mu}-\frac{\beta \boldsymbol{g}(T_2-T_0)}{\nu}. \tag{11}$$

The solution of equations (9)–(11) yields the velocity field. Equations (9)–(11) can be written in a dimensionless form by employing the dimensionless quantities

$$u=\frac{U}{U_0},\quad \theta=\frac{T-T_0}{\Delta T},\quad y=\frac{Y}{D},\quad Gr=\frac{\boldsymbol{g}\beta\Delta T D^3}{\nu^2},$$

$$Re=\frac{U_0 D}{\nu},\quad Pr=\frac{\nu}{\alpha},\quad Br=\frac{\mu U_0^2}{k\Delta T},$$

$$\Xi=\frac{Gr}{Re},\quad R_T=\frac{T_2-T_1}{\Delta T} \tag{12}$$

where $D=2L$ is the hydraulic diameter. The reference velocity U_0 and the reference temperature T_0 are given by

$$U_0=-\frac{AD^2}{48\mu},\quad T_0=\frac{T_1+T_2}{2}. \tag{13}$$

Moreover, the reference temperature difference ΔT is given either by

$$\Delta T=T_2-T_1 \tag{14}$$

if $T_1<T_2$, or by

$$\Delta T=\frac{\nu^2}{c_\mathrm{p}D^2} \tag{15}$$

if $T_1=T_2$. As a consequence, the dimensionless parameter R_T can only assume the values 0 or 1. More precisely, the temperature difference ratio R_T is equal to 1 for asymmetric heating, $T_1<T_2$, while $R_T=0$ for symmetric heating, $T_1=T_2$.

The dimensionless mean velocity $\bar{u}$ and the dimensionless bulk temperature θ_b are given by

$$\bar{u}=2\int_{-1/4}^{1/4}u\,\mathrm{d}y \tag{16}$$

$$\theta_\mathrm{b}=\frac{2}{\bar{u}}\int_{-1/4}^{1/4}u\theta\,\mathrm{d}y. \tag{17}$$

Equation (6) implies that A can be either positive or negative. If $A>0$, then U_0, Re and Ξ are negative, i.e. the flow is downward. On the contrary, if $A<0$, the flow is upward, so that U_0, Re and Ξ are positive. On account of equation (12), equations (9)–(11) can be rewritten as

$$\frac{\mathrm{d}^4u}{\mathrm{d}y^4}=\Xi\,Br\left(\frac{\mathrm{d}u}{\mathrm{d}y}\right)^2 \tag{18}$$

$$u(-1/4)=u(1/4)=0 \tag{19}$$

$$\left.\frac{\mathrm{d}^2u}{\mathrm{d}y^2}\right|_{y=-1/4}=-48+\frac{R_T\Xi}{2},\quad \left.\frac{\mathrm{d}^2u}{\mathrm{d}y^2}\right|_{y=1/4}=-48-\frac{R_T\Xi}{2}. \tag{20}$$

As a consequence of equations (5), (8) and (12), the dimensionless temperature θ can be evaluated either by integrating the equation

$$\frac{d^2\theta}{dy^2}+Br\left(\frac{du}{dy}\right)^2=0 \tag{21}$$

or by the equation

$$\theta=-\frac{1}{\Xi}\left(48+\frac{d^2u}{dy^2}\right). \tag{22}$$

Equations (18)–(22) show that the dimensionless velocity profile and the dimensionless temperature profile depend on three parameters, namely the ratio $\Xi=Gr/Re$, the Brinkman number Br and the temperature difference ratio R_T. A Nusselt number can be defined at each boundary, namely

$$Nu_-=\frac{D}{\Delta T}\frac{dT}{dY}\bigg|_{Y=-L/2},\quad Nu_+=\frac{D}{\Delta T}\frac{dT}{dY}\bigg|_{Y=L/2}. \tag{23}$$

On account of equation (23), it is easily proved that Nu_- and Nu_+ can be employed to evaluate the boundary heat fluxes. Indeed, $-k\Delta TNu_-/D$ and $-k\Delta TNu_+/D$ yield the Y-component of the heat flux density evaluated at $Y=-L/2$ and at $Y=L/2$, respectively. As a consequence of equations (12) and (22), equation (23) can be rewritten as

$$Nu_-=\frac{d\theta}{dy}\bigg|_{y=-1/4}=-\frac{1}{\Xi}\frac{d^3u}{dy^3}\bigg|_{y=-1/4},$$

$$Nu_+=\frac{d\theta}{dy}\bigg|_{y=1/4}=-\frac{1}{\Xi}\frac{d^3u}{dy^3}\bigg|_{y=1/4}. \tag{24}$$

On the other hand, the customary definition of the Nusselt numbers is based on the bulk temperature as the reference fluid temperature, namely

$$\widehat{Nu}_-=\frac{2}{R_T+2\theta_b}\frac{d\theta}{dy}\bigg|_{y=-1/4}=\frac{2Nu_-}{R_T+2\theta_b},$$

$$\widehat{Nu}_+=\frac{2}{R_T-2\theta_b}\frac{d\theta}{dy}\bigg|_{y=1/4}=\frac{2Nu_+}{R_T-2\theta_b}. \tag{25}$$

On account of equations (12) and (25), it is easily proved that $\widehat{Nu}_-$ and $\widehat{Nu}_+$ are such that $k(T_1-T_b)\widehat{Nu}_-/D$ and $k(T_b-T_2)\widehat{Nu}_+/D$ yield the Y-component of the heat flux density evaluated at $Y=-L/2$ and at $Y=L/2$, respectively. However, equation (25) shows that $\widehat{Nu}_-$ and $\widehat{Nu}_+$ are ill-defined if $\theta_b=\pm R_T/2$.

Equation (21) shows that, if the viscous dissipation is negligible so that $Br=0$, the dimensionless temperature θ and the dimensionless velocity u are uncoupled. In this case, equations (18)–(20) can be easily solved and yield

$$u=\left(\frac{\Xi y}{3}R_T+24\right)\left(\frac{1}{16}-y^2\right). \tag{26}$$

Equation (26) corresponds to the velocity profile determined by Aung and Worku [3]. By substituting equation (26) in equations (22) and (24), one obtains

$$\theta=2R_Ty,\quad Nu_-=Nu_+=2R_T. \tag{27}$$

The substitution of equations (26) and (27) in equations (16) and (17) yields $\bar{u}=1$ and $\theta_b=\Xi R_T/2880$. On account of equation (27), when $Br=0$, heat is transferred by pure conduction for asymmetric heating ($R_T=1$), while, for symmetric heating ($R_T=0$), the temperature is uniform and no heat transfer occurs. Both for symmetric heating with an arbitrary value of Ξ and for asymmetric heating with $\Xi=0$, equation (26) yields the usual Hagen–Poiseuille velocity profile. This result is conceivable since, for symmetric heating, equation (27) shows that the temperature is uniform, so that no buoyancy force can be present if viscous dissipation is neglected. Moreover, for asymmetric heating, the hypothesis $\Xi=0$ implies that $Gr=0$, i.e. that buoyancy forces are vanishing.

In the case of asymmetric heating, when buoyancy forces are dominant, i.e. when $\Xi\to\pm\infty$, equations (12) and (26) yield

$$\frac{UD}{\nu\,Gr}=\frac{u}{\Xi}=\left(\frac{y}{3}+\frac{24}{\Xi}\right)\left(\frac{1}{16}-y^2\right)\underset{\Xi\to\pm\infty}{\to}\frac{y}{3}\left(\frac{1}{16}-y^2\right). \tag{28}$$

Equation (28) yields Batchelor's velocity profile for free convection [10].

With $T_1<T_2$ and $U_0>0$ (upward flow), one expects that for a sufficiently high value of Ξ a flow reversal induced by the buoyancy forces occurs at the cool wall $y=-1/4$. On account of equation (26), the critical value Ξ_c such that for $\Xi>\Xi_c$ this flow reversal occurs can be obtained by the condition

$$0=\frac{du}{dy}\bigg|_{y=-1/4}=12-\frac{\Xi_c}{24} \tag{29}$$

i.e. $\Xi_c=288$. For $T_1<T_2$ and $U_0<0$ (downward flow), one expects that there exists a negative critical value Ξ_c of Ξ such that for $\Xi<\Xi_c$ a flow reversal occurs at the hot wall $y=1/4$. In analogy with equation (29), the critical value Ξ_c can be obtained by the relation

$$0=\frac{du}{dy}\bigg|_{y=1/4}=-12-\frac{\Xi_c}{24} \tag{30}$$

i.e. $\Xi_c=-288$. In Fig. 2, plots of u vs y expressed by equation (26) are reported for asymmetric heating ($R_T=1$) with $\Xi=0$, $\Xi=200$ and $\Xi=400$. As expected, the plot with $\Xi=400$ presents a flow reversal near the cool wall $y=-1/4$. As it can be easily inferred from equation (26), the plots of u for $\Xi=-200$ and $\Xi=-400$ are easily obtained from Fig. 2 by performing a reflection of the y-axis.

Another simple solution of equations (18)–(21) can be obtained when buoyancy forces are negligible and viscous dissipation is relevant. In this case, the parameter $\Xi=Gr/Re$ is zero, so that a purely forced convection occurs. Obviously, the Hagen–Poiseuille velocity profile,

$$u=24\left(\frac{1}{16}-y^2\right) \tag{31}$$

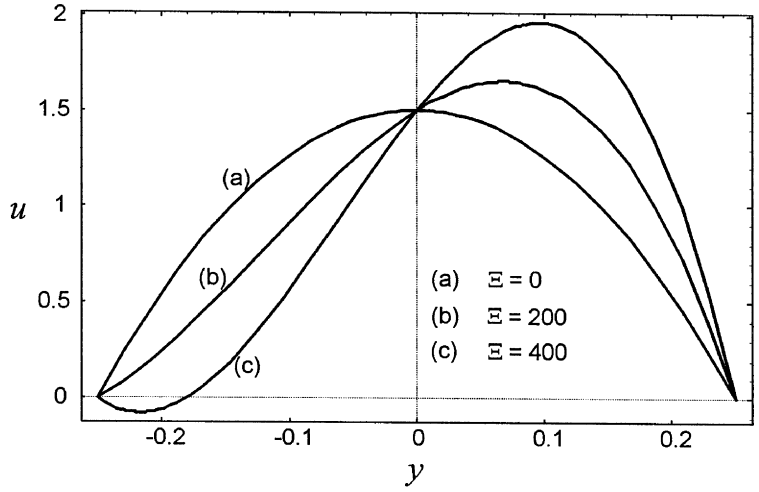

Fig. 2. Plots of u vs y in the case of asymmetric heating, for different values of Ξ and $Br = 0$.

is present within the channel. Indeed, both for symmetric and for asymmetric heating, equation (31) is the solution of equations (18)–(20) when $\Xi = 0$. Since the boundary conditions on θ are $\theta(-1/4) = -R_T/2$ and $\theta(1/4) = R_T/2$, equations (21) and (31) yield

$$\theta = -192Br\,y^4 + 2R_T y + \frac{3Br}{4}. \tag{32}$$

By substituting equations (31) and (32) in equations (16) and (17), one obtains $\bar{a} = 1$ and $\theta_b = 24Br/35$. Equations (24) and (32) yield

$$Nu_- = 2R_T + 12Br, \quad Nu_+ = 2R_T - 12Br \tag{33}$$

while, on account of equations (25) and (33), one obtains

$$\widehat{Nu}_- = 140\frac{R_T + 6Br}{35R_T + 48Br}, \quad \widehat{Nu}_+ = 140\frac{R_T - 6Br}{35R_T - 48Br}. \tag{34}$$

Equations (32) and (34) agree with the results obtained by Cheng and Wu [11] in the case of forced convection with asymmetric heating. For symmetric heating ($R_T = 0$), equation (34) yields $\widehat{Nu}_- = \widehat{Nu}_+ = 35/2$. The same value of $\widehat{Nu}_-$ and $\widehat{Nu}_+$ is obtained for asymmetric heating with $Br \to \infty$. Equation (33) reveals that, for asymmetric heating with $Br < 1/6$, the wall heat flux at $y = 1/4$ is directed inside the channel, while at $y = -1/4$ is directed outside the channel. On the other hand, for asymmetric heating with $Br > 1/6$ and for symmetric heating with any nonzero value of Br, the wall heat flux is directed outside the channel both at $y = 1/4$ and at $y = -1/4$. In Fig. 3, plots of θ vs y expressed by equation (32) are reported for asymmetric heating ($R_T = 1$) with $Br = 0$, $Br = 2$ and $Br = 4$. This figure shows that, although the conduction regime holds only for $Br = 0$, there exists a region around $y = 0$ where θ is approximately a linear function of y also for $Br \neq 0$.

3. Perturbation method

In this section, equations (18)–(20) are solved by a perturbation series method. Then, equation (22) is employed to determine the dimensionless temperature field.

Let us define the dimensionless parameter

$$\varepsilon = Br\,\Xi = Re\,Pr\frac{\beta g D}{c_p}. \tag{35}$$

Equation (35) shows that ε does not depend on the reference temperature difference ΔT. It is easily verified that, for a fixed value of $\Xi \neq 0$, the solution of equations (18)–(20) can be expressed by the perturbation expansion

$$u(y) = u_0(y) + u_1(y)\varepsilon + u_2(y)\varepsilon^2 + \cdots = \sum_{n=0}^{\infty} u_n(y)\varepsilon^n. \tag{36}$$

The perturbation method solution of equations (18)–(20) is as follows [12]. First, one substitutes equation (36) in equations (18)–(20) and collects terms having like powers of ε. Then, one equates the coefficient of each power of ε to zero. Finally, one is led to a sequence of boundary value problems which can be solved in succession to obtain the unknown functions $u_n(y)$.

For $n = 0$, one obtains the boundary value problem

$$\frac{d^4 u_0}{dy^4} = 0 \tag{37}$$

$$u_0(-1/4) = u_0(1/4) = 0 \tag{38}$$

$$\left.\frac{d^2 u_0}{dy^2}\right|_{y=-1/4} = -48 + R_T\frac{\Xi}{2}, \quad \left.\frac{d^2 u_0}{dy^2}\right|_{y=1/4} = -48 - R_T\frac{\Xi}{2}. \tag{39}$$

The solution of equations (37)–(39) is given by

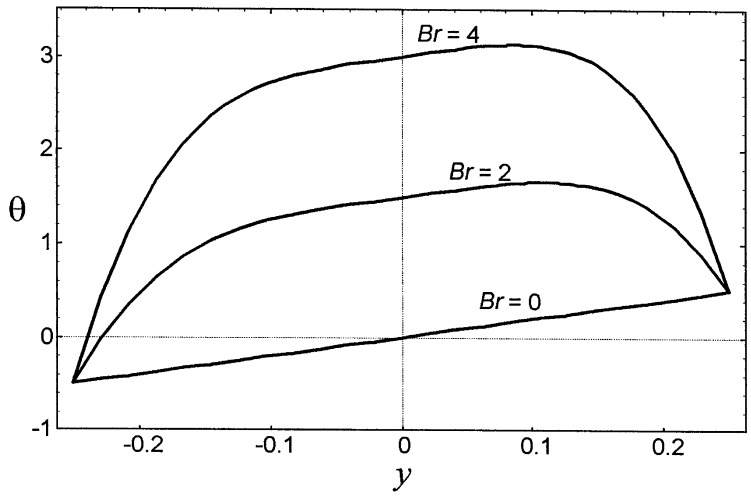

Fig. 3. Plots of θ vs y in the case of asymmetric heating, for different values of Br and $\Xi = 0$.

$$u_0(y) = \left(\frac{\Xi y}{3} R_T + 24\right)\left(\frac{1}{16} - y^2\right). \tag{40}$$

Obviously, the right-hand side of equation (40) coincides with the dimensionless velocity profile in the case $Br = 0$, as it can be checked by a comparison with the right hand side of equation (26). On account of equations (18)–(20) and (36), one obtains the following boundary value problem fulfilled by the unknown functions $u_n(y)$, for every integer $n > 0$:

$$\frac{\mathrm{d}^4 u_n}{\mathrm{d}y^4} = \sum_{j=0}^{n-1} \frac{\mathrm{d}u_j}{\mathrm{d}y}\frac{\mathrm{d}u_{n-j-1}}{\mathrm{d}y} \tag{41}$$

$$u_n(-1/4) = u_n(1/4) = 0 \tag{42}$$

$$\left.\frac{\mathrm{d}^2 u_n}{\mathrm{d}y^2}\right|_{y=-1/4} = \left.\frac{\mathrm{d}^2 u_n}{\mathrm{d}y^2}\right|_{y=1/4} = 0. \tag{43}$$

Equation (40) and the iterative solution of equations (41)–(43) allow one to determine the functions $u_n(y)$. Then, on account of equations (22), (36) and (40), the dimensionless temperature θ can be expressed as

$$\theta(y) = 2R_T y - \frac{1}{\Xi}\sum_{n=1}^{\infty} \frac{\mathrm{d}^2 u_n(y)}{\mathrm{d}y^2}\varepsilon^n. \tag{44}$$

The Nusselt numbers Nu_- and Nu_+ can be evaluated by employing equations (24) and (44), namely

$$Nu_- = 2R_T + \sum_{n=1}^{\infty} a_n \varepsilon^n \tag{45}$$

$$Nu_+ = 2R_T + \sum_{n=1}^{\infty} b_n \varepsilon^n \tag{46}$$

where the coefficients a_n and b_n are given by

$$a_n = -\frac{1}{\Xi}\left.\frac{\mathrm{d}^3 u_n}{\mathrm{d}y^3}\right|_{y=-1/4}, \quad b_n = -\frac{1}{\Xi}\left.\frac{\mathrm{d}^3 u_n}{\mathrm{d}y^3}\right|_{y=1/4}. \tag{47}$$

On account of equations (16), (17), (36) and (44), the mean dimensionless velocity $\bar{u}$ and the bulk value of the dimensionless temperature θ_b can be expressed as

$$\bar{u} = 1 + \sum_{n=1}^{\infty} c_n \varepsilon^n \tag{48}$$

$$\theta_b = \frac{48}{\Xi}\left(\frac{1}{\bar{u}} - 1\right) + \frac{\Xi R_T}{2880\bar{u}} + \frac{1}{\bar{u}}\sum_{n=1}^{\infty} d_n \varepsilon^n \tag{49}$$

where the coefficients c_n and d_n are given by

$$c_n = 2\int_{-1/4}^{1/4} u_n(y)\,\mathrm{d}y \tag{50}$$

$$d_n = \frac{2}{\Xi}\sum_{j=0}^{n}\int_{-1/4}^{1/4} \frac{\mathrm{d}u_j(y)}{\mathrm{d}y}\frac{\mathrm{d}u_{n-j}(y)}{\mathrm{d}y}\mathrm{d}y. \tag{51}$$

As a consequence of equations (47) and (51), an integration of both sides of equation (41) with respect to y in the interval $[-1/4, 1/4]$ yields a relation between the coefficients a_n, b_n and d_n, namely

$$d_n = 2(a_{n+1} - b_{n+1}). \tag{52}$$

4. Asymmetric heating

In this section, the perturbation method described in the preceding section is employed to analyse the case of asymmetric heating ($R_T = 1$).

When the boundary temperatures T_1 and T_2 are different, both the dimensionless velocity u and the dimensionless temperature θ depend on the dimensionless parameters ε and Ξ. When the flow is upward, ε and Ξ are positive. On the other hand, when the flow is downward, ε and Ξ are negative. Although the sign of ε and that of

Table 1
Values of the coefficients a_n, b_n, c_n and d_n for asymmetric heating with $\Xi = 100$ and $\Xi = 500$

	$\Xi = 100$				$\Xi = 500$			
n	a_n	$-b_n$	c_n	d_n	a_n	$-b_n$	c_n	d_n
1	9.535×10^{-2}	1.620×10^{-1}	1.558×10^{-2}	1.504×10^{-2}	3.407×10^{-2}	1.007×10^{-1}	4.658×10^{-2}	9.357×10^{-3}
2	3.235×10^{-3}	4.284×10^{-3}	4.688×10^{-4}	5.683×10^{-4}	8.989×10^{-4}	3.779×10^{-3}	1.492×10^{-3}	5.121×10^{-4}
3	1.263×10^{-4}	1.578×10^{-4}	1.785×10^{-5}	2.422×10^{-5}	7.858×10^{-5}	1.775×10^{-4}	8.265×10^{-5}	2.987×10^{-5}
4	5.455×10^{-6}	6.653×10^{-6}	7.633×10^{-7}	1.108×10^{-6}	4.732×10^{-6}	1.020×10^{-5}	4.794×10^{-6}	1.911×10^{-6}
5	2.515×10^{-7}	3.027×10^{-7}	3.500×10^{-8}	5.320×10^{-8}	3.185×10^{-7}	6.368×10^{-7}	3.069×10^{-7}	1.277×10^{-7}
6	1.213×10^{-8}	1.447×10^{-8}	1.682×10^{-9}	2.642×10^{-9}	2.173×10^{-8}	4.212×10^{-8}	2.051×10^{-8}	8.857×10^{-9}
7	6.043×10^{-10}	7.169×10^{-10}	8.364×10^{-11}	1.347×10^{-10}	1.533×10^{-9}	2.896×10^{-9}	1.422×10^{-9}	6.304×10^{-10}
8	3.087×10^{-11}	3.646×10^{-11}	4.265×10^{-12}	7.002×10^{-12}	1.103×10^{-10}	2.049×10^{-10}	1.012×10^{-10}	4.580×10^{-11}
9	1.608×10^{-12}	1.893×10^{-12}	2.219×10^{-13}	3.699×10^{-13}	8.085×10^{-12}	1.482×10^{-11}	7.357×10^{-12}	3.383×10^{-12}
10	8.506×10^{-14}	9.990×10^{-14}	1.173×10^{-14}	1.981×10^{-14}	6.012×10^{-13}	1.090×10^{-12}	5.434×10^{-13}	2.532×10^{-13}
11	4.559×10^{-15}	5.344×10^{-15}	6.280×10^{-16}	1.072×10^{-15}	4.525×10^{-14}	8.138×10^{-14}	4.068×10^{-14}	1.917×10^{-14}
12	2.470×10^{-16}	2.890×10^{-16}	3.400×10^{-17}	5.858×10^{-17}	3.441×10^{-15}	6.145×10^{-15}	3.080×10^{-15}	1.465×10^{-15}
13	1.351×10^{-17}	1.578×10^{-17}	1.858×10^{-18}	3.226×10^{-18}	2.639×10^{-16}	4.687×10^{-16}	2.354×10^{-16}	1.129×10^{-16}
14	7.444×10^{-19}	8.687×10^{-19}	1.024×10^{-19}	1.789×10^{-19}	2.040×10^{-17}	3.605×10^{-17}	1.814×10^{-17}	8.761×10^{-18}
15	4.131×10^{-20}	4.816×10^{-20}	5.679×10^{-21}	9.985×10^{-21}	1.587×10^{-18}	2.793×10^{-18}	1.408×10^{-18}	6.840×10^{-19}
16	2.306×10^{-21}	2.686×10^{-21}	3.169×10^{-22}	5.602×10^{-22}	1.242×10^{-19}	2.178×10^{-19}	1.099×10^{-19}	5.370×10^{-20}
17	1.295×10^{-22}	1.507×10^{-22}	1.778×10^{-23}	3.158×10^{-23}	9.771×10^{-21}	1.708×10^{-20}	8.628×10^{-21}	4.236×10^{-21}
18	7.301×10^{-24}	8.490×10^{-24}	1.003×10^{-24}	1.788×10^{-24}	7.722×10^{-22}	1.346×10^{-21}	6.807×10^{-22}	3.356×10^{-22}
19	4.135×10^{-25}	4.805×10^{-25}	5.677×10^{-26}	1.016×10^{-25}	6.128×10^{-23}	1.065×10^{-22}	5.393×10^{-23}	2.670×10^{-23}
20	2.351×10^{-26}	2.730×10^{-26}	3.227×10^{-27}	5.796×10^{-27}	4.881×10^{-24}	8.467×10^{-24}	4.290×10^{-24}	2.131×10^{-24}

Ξ are constrained to be equal, their absolute values are independent.

In Table 1, the first 20 coefficients, a_n, b_n, c_n and d_n defined by equations (47), (50) and (51) are evaluated for $\Xi = 100$ and $\Xi = 500$. In Table 2, the values of the Nusselt numbers Nu_-, Nu_+, $\widehat{Nu}_-$ and $\widehat{Nu}_+$ are reported for $\Xi = 100$ and $\Xi = 500$. To obtain the values reported in Table 2, the first 20 terms of the perturbation series are sufficient when $\Xi = 100$, while the first 30 terms are necessary for the computation when $\Xi = 500$.

The values of a_n, b_n, c_n and d_n reported in Table 1 refer to upward flows. However, as is shown in the following, the values reported in Table 1 can also be employed to evaluate a_n, b_n, c_n and d_n for downward flow with $\Xi = -100$ and $\Xi = -500$. Indeed, the dimensionless velocity u is determined by equations (18)–(20). It is easily

Table 2
Values of Nu_-, Nu_+, $\widehat{Nu}_-$ and $\widehat{Nu}_+$ for asymmetric heating with $\Xi = 100$ and $\Xi = 500$

	$\Xi = 100$				$\Xi = 500$			
ε	Nu_-	Nu_+	$\widehat{Nu}_-$	$\widehat{Nu}_+$	Nu_-	Nu_+	$\widehat{Nu}_-$	$\widehat{Nu}_+$
0	2.000	2.000	3.740	4.299	2.000	2.000	2.969	6.128
0.5	2.048	1.918	3.806	4.154	2.017	1.949	3.002	5.942
1	2.099	1.834	3.872	4.003	2.035	1.895	3.034	5.755
2	2.205	1.657	4.011	3.681	2.072	1.782	3.101	5.371
3	2.319	1.471	4.156	3.327	2.113	1.658	3.171	4.970
4	2.443	1.271	4.309	2.935	2.157	1.522	3.244	4.544
5	2.578	1.058	4.471	2.498	2.207	1.370	3.321	4.084
6	2.726	0.828	4.642	2.005	2.264	1.200	3.406	3.577
7	2.889	0.578	4.825	1.441	2.331	1.004	3.502	3.003
8	3.070	0.305	5.022	0.786	2.414	0.773	3.612	2.330
9	3.275	0.004	5.234	0.011	2.520	0.490	3.748	1.497
10	3.508	−0.332	5.465	−0.928	2.671	0.119	3.930	0.370

verified that, when $R_T = 1$, these equations are invariant under the transformation

$$u \to u, \quad \varepsilon \to \varepsilon, \quad \Xi \to -\Xi, \quad y \to -y. \tag{53}$$

This symmetry is purely mathematical, since, as it has been pointed out above, it is physically meaningless to keep ε fixed while the sign of Ξ is reversed. As a consequence of equation (36) and of the symmetry of equations (18)–(20) expressed by equation (53), the flow reversal transformation $\Xi \to -\Xi$ implies $u_n(y) \to u_n(-y)$. Then, on account of equations (47), (50) and (51), the flow reversal transformation $\Xi \to -\Xi$ yields $a_n \to b_n$, $b_n \to a_n$, $c_n \to c_n$ and $d_n \to -d_n$.

In Table 3, the Nusselt numbers Nu_-, Nu_+, $\widehat{Nu}_-$ and $\widehat{Nu}_+$ are reported for $\Xi = -100$ and $\Xi = -500$. As in the corresponding cases of upward flow, the first 20 terms of the perturbation series are employed for the computation when $\Xi = -100$, while the first 30 terms are necessary when $\Xi = -500$.

Tables 2 and 3 show that heat transfer is enhanced at $y = -1/4$ when the modulus of ε is increased, since both Nu_- and $\widehat{Nu}_-$ increase. On the other hand, both Nu_+ and $\widehat{Nu}_+$ are decreasing functions of the modulus of ε. This behaviour of the heat transfer coefficient is exhibited for upward as well as for downward flow. In particular, when $\Xi = 100$, Nu_+ and $\widehat{Nu}_+$ are zero for a value of ε in the interval $9 < \varepsilon < 10$ and for greater values of ε they become negative. This sign change of Nu_+ and $\widehat{Nu}_+$ is due to the change of direction of the heat flux density vector at the hot wall when viscous dissipation is sufficiently relevant.

In Fig. 4, plots of u and θ in the case $\Xi = 100$ are reported for $\varepsilon = 0$, $\varepsilon = 8$ and $\varepsilon = 12$. The first 20 terms of the perturbation series are sufficient to obtain these plots. Figure 4 shows that the dimensionless velocity and the dimensionless temperature at each position are increasing functions of ε. This behaviour can be explained as follows. A greater energy generated by viscous dissipation yields a greater fluid temperature and, as a consequence, a greater buoyancy force. The increase of the buoyancy force implies an increase of the velocity in the upward direction.

In Fig. 5, the case $\Xi = 500$ is considered. The plots of u for $\varepsilon = 0$ and $\varepsilon = 8$ display a flow reversal close to the boundary $y = -1/4$, while no flow reversal is present in the plot for $\varepsilon = 12$. Indeed, viscous dissipation tends to increase the buoyancy force at each position and, as a consequence, it tends to contrast the flow reversal at the cool wall.

Figures 6 and 7 refer to $\Xi = -100$ and $\Xi = -500$, respectively. The plots of u and θ reported in these figures reveal that, if the Brinkman number is increased, u decreases and θ increases. However, the change of the dimensionless temperature due to viscous dissipation is not so sensible as in the case of upward flow. Figure 7 shows that the flow reversal next to the hot wall becomes stronger as Br increases. Indeed, the behaviour of the dimensionless velocity profile for increasing values of Br is explained again by the increase of the buoyancy forces.

5. Symmetric heating

In this section, the perturbation method is employed to study the velocity profiles and the temperature profiles in the case of symmetric heating ($R_T = 0$).

When the boundary temperatures T_1 and T_2 are equal, equations (18)–(20) show that the dimensionless velocity u is a symmetric function of y which depends only on the dimensionless parameter ε. Therefore, on account of equation (22), also θ is a symmetric function of y and is

Table 3
Values of Nu_-, Nu_+, $\widehat{Nu}_-$ and $\widehat{Nu}_+$ for asymmetric heating with $\Xi = -100$ and $\Xi = -500$

	$\Xi = -100$				$\Xi = -500$			
$-\varepsilon$	Nu_-	Nu_+	$\widehat{Nu}_-$	$\widehat{Nu}_+$	Nu_-	Nu_+	$\widehat{Nu}_-$	$\widehat{Nu}_+$
0	2.000	2.000	4.299	3.740	2.000	2.000	6.128	2.969
0.5	2.080	1.953	4.437	3.676	2.049	1.983	6.311	2.937
1	2.158	1.908	4.571	3.614	2.097	1.967	6.494	2.905
2	2.308	1.821	4.823	3.492	2.188	1.935	6.859	2.841
3	2.451	1.740	5.059	3.376	2.272	1.904	7.227	2.777
4	2.588	1.663	5.278	3.264	2.352	1.874	7.602	2.713
5	2.719	1.591	5.485	3.156	2.427	1.845	7.991	2.649
6	2.845	1.523	5.679	3.051	2.497	1.815	8.397	2.584
7	2.966	1.458	5.863	2.951	2.564	1.786	8.829	2.517
8	3.083	1.396	6.036	2.853	2.627	1.757	9.295	2.450
9	3.195	1.337	6.201	2.759	2.687	1.728	9.805	2.380
10	3.304	1.281	6.358	2.667	2.743	1.699	10.374	2.310

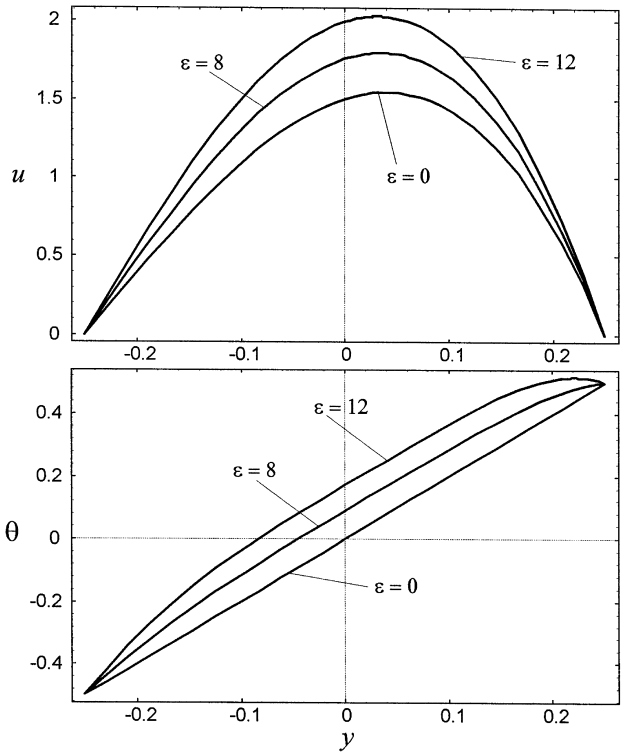

Fig. 4. Plots of u and θ vs y in the case of asymmetric heating, for different values of ε and $\Xi = 100$.

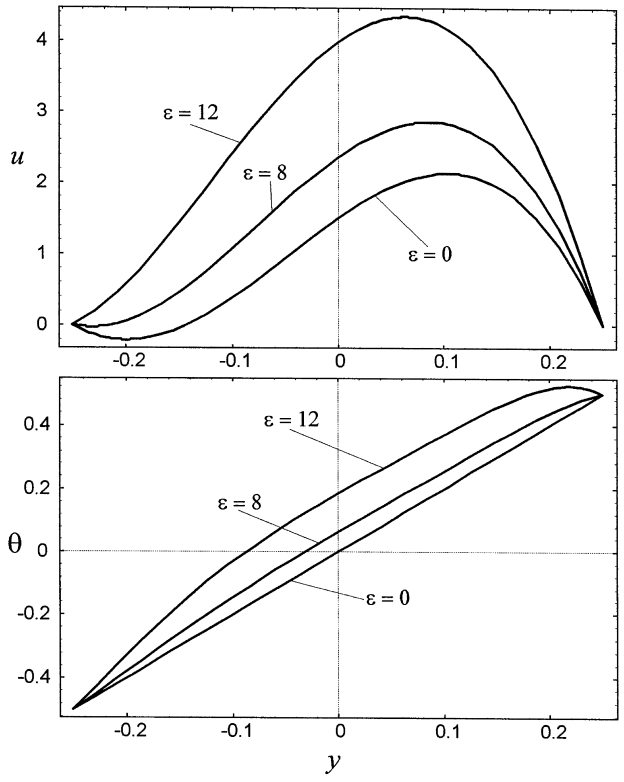

Fig. 5. Plots of u and θ vs y in the case of asymmetric heating, for different values of ε and $\Xi = 500$.

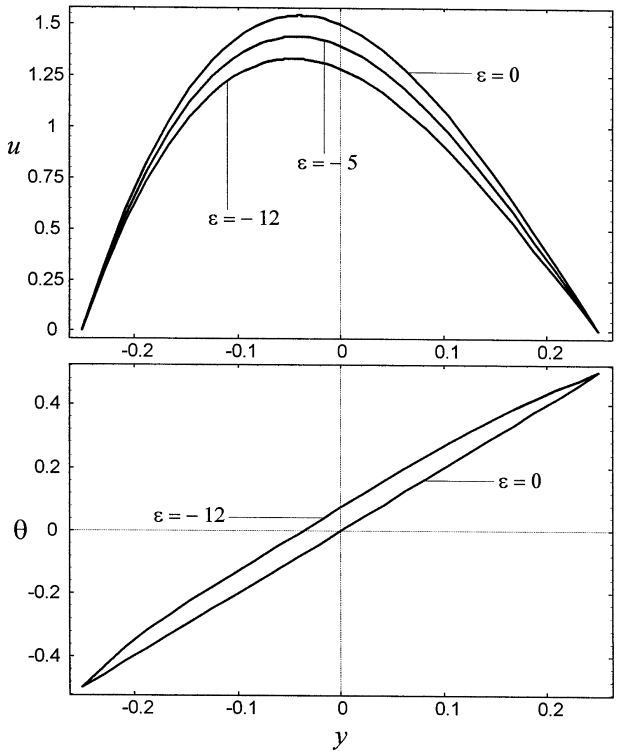

Fig. 6. Plots of u and θ vs y in the case of asymmetric heating, for different values of ε and $\Xi = -100$.

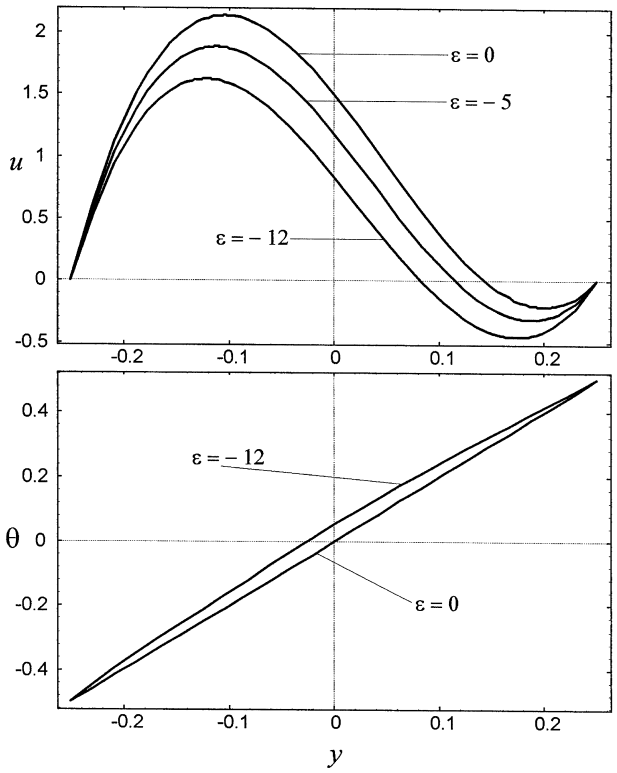

Fig. 7. Plots of u and θ vs y in the case of asymmetric heating, for different values of ε and $\Xi = -500$.

such that $\Xi\theta$ depends only on ε. Equation (36) ensures that the symmetry of u implies the symmetry of $u_n(y)$ for every $n \geqslant 0$. Moreover, functions $u_n(y)$ do not depend on Ξ. As a consequence of the symmetry of θ and of $u_n(y)$, equations (24), (25) and (47) imply that $Nu_+ = -Nu_-$, $\widehat{Nu}_+ = \widehat{Nu}_-$ and $b_n = -a_n$. Equations (24) and (25) ensure that ΞNu_- and $\widehat{Nu}_-$ are uniquely determined by ε, while equations (47), (50) and (51) show that Ξa_n, c_n and Ξd_n do not depend on Ξ. As in the case of asymmetric heating, both ε and Ξ are positive when the flow is upward, while they are negative when the flow is downward.

In Table 4, the first 20 coefficients Ξa_n, c_n and Ξd_n are evaluated. In Table 5, the values of ΞNu_- and $\widehat{Nu}_-$ are reported in the range $-10 \leqslant \varepsilon \leqslant 10$. To obtain the values reported in Table 5, the first 20 terms of the perturbation series are sufficient. The value of $\widehat{Nu}_-$ for $\varepsilon = 0$ is obtained as a limit for $\varepsilon \to 0$ and coincides with that given by equation (34) when $R_T = 0$, i.e. $35/2 = 17.5$.

In Fig. 8, the velocity u and the product $\Xi\theta$ are plotted vs y for some values of ε in the range $-12 \leqslant \varepsilon \leqslant 12$. This figure shows that the effect of viscous dissipation on the dimensionless velocity profile and on the dimensionless temperature profile is more significant in the case of upward flow ($\varepsilon > 0$) than in the case of downward flow ($\varepsilon < 0$). This behaviour is similar to that observed in the case of asymmetric heating. Moreover, Fig. 8 shows that, if ε increases, at any given position both u and $\Xi\theta$ increase. As in the case of asymmetric heating, this behaviour can be explained by the increase of the energy generated by viscous dissipation which yields a greater fluid temperature and, as a consequence, a greater buoyancy force. The increase of the buoyancy force implies an increase of the dimensionless velocity, in the case of upward flow, and a decrease of the dimensionless velocity, in the case of downward flow.

Table 4
Values of the coefficients Ξa_n, c_n and Ξd_n for symmetric heating

n	Ξa_n	c_n	Ξd_n
1	12	1.429×10^{-2}	1.371
2	3.429×10^{-1}	4.261×10^{-4}	5.075×10^{-2}
3	1.269×10^{-2}	1.591×10^{-5}	2.114×10^{-3}
4	5.286×10^{-4}	6.654×10^{-7}	9.455×10^{-5}
5	2.364×10^{-5}	2.982×10^{-8}	4.433×10^{-6}
6	1.108×10^{-6}	1.400×10^{-9}	2.150×10^{-7}
7	5.376×10^{-8}	6.797×10^{-11}	1.070×10^{-8}
8	2.675×10^{-9}	3.385×10^{-12}	5.432×10^{-10}
9	1.358×10^{-10}	1.719×10^{-13}	2.802×10^{-11}
10	7.006×10^{-12}	8.873×10^{-15}	1.465×10^{-12}
11	3.662×10^{-13}	4.640×10^{-16}	7.741×10^{-14}
12	1.935×10^{-14}	2.453×10^{-17}	4.129×10^{-15}
13	1.032×10^{-15}	1.309×10^{-18}	2.220×10^{-16}
14	5.551×10^{-17}	7.038×10^{-20}	1.202×10^{-17}
15	3.006×10^{-18}	3.811×10^{-21}	6.549×10^{-19}
16	1.637×10^{-19}	2.077×10^{-22}	3.587×10^{-20}
17	8.968×10^{-21}	1.138×10^{-23}	1.974×10^{-21}
18	4.935×10^{-22}	6.261×10^{-25}	1.091×10^{-22}
19	2.728×10^{-23}	3.461×10^{-26}	6.054×10^{-24}
20	1.513×10^{-24}	1.920×10^{-27}	3.371×10^{-25}

Table 5
Values of ΞNu_- and $\widehat{Nu}_-$ for symmetric heating

ε	ΞNu_-	$\widehat{Nu}_-$
−10	−94.730	17.704
−9	−86.994	17.685
−8	−78.952	17.667
−7	−70.582	17.647
−6	−61.856	17.628
−5	−52.744	17.608
−4	−43.211	17.587
−3	−33.219	17.566
−2	−22.722	17.545
−1	−11.669	17.523
−0.5	−5.916	17.511
0	0	17.500
0.5	6.087	17.488
1	12.356	17.477
2	25.482	17.452
3	39.478	17.427
4	54.463	17.401
5	70.584	17.374
6	88.025	17.346
7	107.017	17.316
8	127.857	17.285
9	150.944	17.252
10	176.819	17.217

6. Conclusions

The laminar and fully developed mixed convection in a plane vertical channel has been analyzed by taking into account the effect of viscous dissipation. The flow has been assumed to be parallel and each of the two boundary planes has been considered as isothermal. The governing equations have been written in a dimensionless form which is appropriate both for the case of different boundary temperatures (asymmetric heating) and for the case of equal boundary temperatures (symmetric heating). The solution of the dimensionless equations has been determined by a perturbation series method which employs $Br\,Gr/Re$ as the perturbation parameter. Dimensionless coefficients suitable for the evaluation of the dimensionless mean velocity, of the dimensionless bulk temperature and of the Nusselt numbers have been tabulated. The dimensionless velocity, the dimensionless temperature and the Nusselt numbers have been evaluated

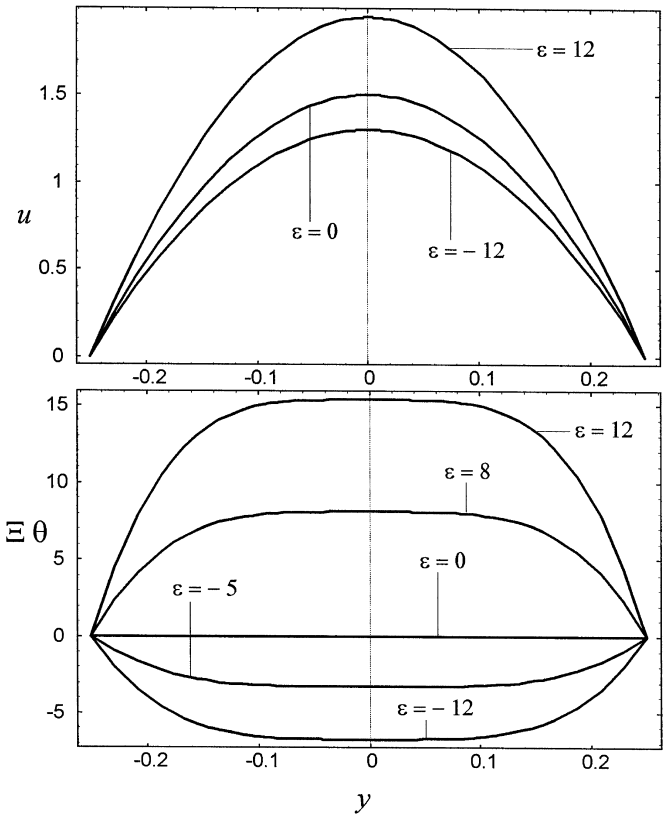

Fig. 8. Plots of u and $\Xi\theta$ vs y in the case of symmetric heating, for different values of ε.

both in the case of asymmetric heating and in the case of symmetric heating. It has been shown that the effect of viscous dissipation can be important especially in the case of upward flow. One of the consequences of the viscous dissipation term in the energy equation is that the heat transfer between the two boundaries of the channel is not simply due to pure conduction as in the case of negligible viscous dissipation. Moreover, for asymmetric heating, it has been shown that viscous dissipation enhances the effect of flow reversal in the case of downward flow, while it lowers this effect in the case of upward flow. In fact, viscous dissipation increases the buoyancy forces and, as a consequence, the fluid velocity in the upward direction.

Acknowledgement

The author is grateful to Professor Enzo Zanchini for helpful discussions on some of the topics treated in this paper.

References

[1] Aung W. Mixed convection in internal flow. In: Kakaç S, Shah RK, Aung W, editors. Handbook of Single-Phase Convective Heat Transfer. New York: Wiley, 1987, Chap. 15.

[2] Tao LN. On combined free and forced convection in channels. ASME Journal of Heat Transfer 1960;82:233–8.

[3] Aung W, Worku G. Theory of fully developed, combined convection including flow reversal. ASME Journal of Heat Transfer 1986;108:485–8.

[4] Cheng C-H, Kou H-S, Huang W-H. Flow reversal and heat transfer of fully developed mixed convection in vertical channels. Journal of Thermophysics and Heat Transfer 1990;4:375–83.

[5] Hamadah TT, Wirtz RA. Analysis of laminar fully developed mixed convection in a vertical channel with opposing buoyancy. ASME Journal of Heat Transfer 1991;113:507–10.

[6] Aung W, Worku G. Developing flow and flow reversal in a vertical channel with asymmetric wall temperatures. ASME Journal of Heat Transfer 1986;108:299–304.

[7] Aung W, Worku G. Mixed convection in ducts with asymmetric wall heat fluxes. ASME Journal of Heat Transfer 1987;109:947–51.

[8] Ingham DB, Keen DJ, Heggs PJ. Flows in vertical channels with asymmetric wall temperatures and including situations where reverse flows occur. ASME Journal of Heat Transfer 1988;110:910–7.

[9] Arpaci VS, Larsen PS. Convection Heat Transfer. Englewood Cliffs, NJ: Prentice-Hall, 1984. pp. 51–4.

[10] Batchelor GK. Heat transfer by free convection across a closed cavity between vertical boundaries at different temperatures. Quarterly of Applied Mathematics 1954;12:209–33.
[11] Cheng KC, Wu R-S. Viscous dissipation effects on convective instability and heat transfer in plane Poiseuille flow heated from below. Applied Scientific Research 1976;32:327–46.
[12] Aziz A, Na TY. Perturbation Methods in Heat Transfer, 1st ed. New York : Hemisphere, 1984.